APPLIED PHYSICS LETTERS 108, 041910 (2016)

# Energy bandgap variation in oblique angle-deposited indium tin oxide

Kyurin Kim,[1] Jun Hyuk Park,[2] Hyunsoo Kim,[1] Jong Kyu Kim,[2] E. Fred Schubert,[3] and Jaehee Cho[1,a)]
[1]*School of Semiconductor and Chemical Engineering, Semiconductor Physics Research Center, Chonbuk National University, Jeonju 561-756, South Korea*
[2]*Department of Materials Science and Engineering, Pohang University of Science and Technology, Pohang 54896, South Korea*
[3]*Future Chips Constellation, Department of Electrical, Computer, and Systems Engineering, Rensselaer Polytechnic Institute, Troy, New York 12180, USA*

(Received 10 November 2015; accepted 18 January 2016; published online 28 January 2016)

Indium tin oxide (ITO) thin films deposited using the oblique angle deposition (OAD) technique exhibit a strong correlation between structural and optical properties, especially the optical bandgap energy. The microstructural properties of ITO thin films are strongly influenced by the tilt angle used during the OAD process. When changing the tilt angle, the refractive index, porosity, and optical bandgap energy of ITO films also change due to the existence of a preferential growth direction at the interface between ITO and the substrate. Experiments reveal that the ITO film's optical bandgap varies from 3.98 eV (at normal incident deposition) to 3.87 eV (at a 60° tilt angle).
 [http://dx.doi.org/10.1063/1.4940998]

Oblique angle deposition (OAD) has emerged as an invaluable technique for the deposition of nanostructured thin film materials.[1] The incorporation of OAD thin films in a variety of device applications is a clear indication of their maturity and excellent potential for advanced device characteristics.[2–10] OAD is generally associated with physical vapor deposition of thin films (prepared through, e.g., electron-beam or thermal evaporation), in which the material vapor flux arrives at the substrate surface at an oblique angle. Tilted and columnar nanostructures are the most typical morphological characteristics of OAD thin films.[1,5,11] An important consequence of the OAD process is that the porosity and optical constants of the nanostructured OAD thin films vary with the degree of obliqueness of the deposition angle.[5,11,12] However, contrary to the well-understood and intensely studied properties of OAD thin films such as the structural, mechanical, and optical characteristics, the effect of OAD process on the *optical bandgap energy* of OAD thin films has been rarely reported. In this article, we investigate indium tin oxide (ITO) thin films deposited using the OAD technique and find a strong correlation between the ITO thin film's structural properties and optical properties, especially the optical bandgap energy.

Deposition of ITO films on soda lime glass and silicon substrates was conducted with an E-beam evaporation system using an ITO source composed of 90 wt. % $In_2O_3$ and 10 wt. % $SnO_2$. Prior to the deposition, all substrates were sequentially cleaned in acetone, isopropyl alcohol, and deionized water and dried under nitrogen flow. The apparatus used in our OAD process has a sample stage (onto which the substrate was loaded), allowing for control of the polar-angle as well as azimuthal rotation. The distance between the substrate and evaporation source material was approximately 50 cm. The sample stage was positioned at a fixed polar angle so that the substrate had a certain tilt angle (deposition angle) with respect to the vapor-flux direction. The chamber was evacuated to a pressure less than $1.0 \times 10^{-6}$ Torr, and substrates were held at room temperature. During the deposition, the deposition rate was held steady at 0.2 nm/s, as measured by a quartz crystal monitor inside the chamber. The low growth rate on the substrate at higher deposition angles[11] was compensated by increasing the deposition time to keep the same film thickness for all samples. The ITO films unloaded from the E-beam evaporation system were annealed in $O_2$ at 550 °C for 1 min in a rapid thermal annealing system in order to compensate a deficiency of oxygen in the films.

Optical transmittance measurements of the ITO thin films were performed using non-polarized light at normal incidence in the wavelength range of 280–780 nm using a JASCO UV-VIS spectrophotometer. The refractive index ($n$) was measured using a spectroscopic ellipsometry system, in which absorption is neglected during fitting. A film thickness was measured first by ellipsometry, and then confirmed by a scanning electron microscope (SEM, Hitachi S-4300). The porosity and optical bandgap energy values of the ITO thin films were calculated using theoretical models developed by Poxson *et al.*[11] and Tauc,[13] respectively. The morphological features of the films were examined using an optical microscope and SEM. Several regions on the sample surface were investigated in order to produce representative images. Furthermore, the crystallographic structure of the ITO thin films was examined by X-ray diffraction (XRD) using the nickel-filtered Kα emission of copper.

Figures 1(a) and 1(b) show optical microscope images of the ITO films deposited on (a) silicon (Si) and (b) glass substrates at tilt angles ranging from 0° to 60°. A color difference of the ITO thin films is clearly evident, which can result from a variation in thickness and/or refractive index. In this case, because the thicknesses of all films are the same (about 210 nm), the variation in refractive index is the cause for the color variation. It is well known that the refractive index of a

a)E-mail: jcho@chonbuk.ac.kr

 

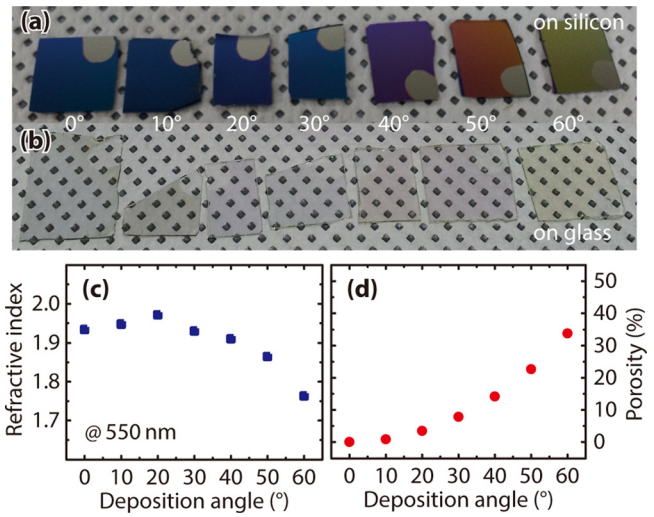


FIG. 1. Optical microscopy images of the ITO thin films on (a) silicon and (b) soda-lime glass substrates. (c) Refractive index and (d) porosity values of the ITO thin films as a function of deposition angle.

thin film material can be tuned based on the porous nanostructure formed by using the OAD technique.[1,3,5,11,12] Figures 1(c) and 1(d) show the refractive index and porosity, respectively, of the ITO films prepared using different tilt angles. The refractive index is measured with a spectroscopic ellipsometry system using ITO films deposited on Si substrates. The refractive indices of the ITO films range from 1.76 to 1.97 and show a decrease with increasing deposition angle when the tilt angle is greater than 20°. The porosity ($p$) of the ITO films can be estimated from the following equation:[11]

$$p = \frac{\theta \tan\theta}{c + \theta \tan\theta}, \tag{1}$$

where $\theta$ is the tilt angle defined as the angle between the substrate normal and the vapor-flux direction, and $c$ denotes a fitting parameter ($c = 3.55$ for ITO).[11] We note that the porosity can be determined from (i) the refractive index or (ii) from Eq. (1). Both methods are in good agreement. The porosity of the ITO films increases with the increasing tilt angle, showing a strong anti-correlation with the refractive index of the film. The maximum porosity is approximately 33.8% for ITO deposited at a tilt angle of 60°.

Figure 2 shows the optical transmittance spectra as a function of wavelength in the range of 280–780 nm for the ITO thin films. No significant difference in transmittance is observed, with all ITO films showing transmittances in the range of 80%–90% for wavelengths greater than 400 nm. The transmittance peak, marked by the arrow in Fig. 2, and the valley (at slightly longer wavelength) move to shorter wavelengths as the tilt angle increases because of the change in refractive index. The SEM images in Fig. 2 show an obvious difference in the microstructures of the ITO films deposited at low and high tilt angles. In the case of the low tilt angles (0° and 10°), the deposited ITO films show a smooth surface and featureless cross-sectional images. However, for the high tilt angles (50° and 60°), the ITO films show a spotty surface and a columnar cross-sectional structure. The results indicate that the change in microstructure of the ITO films directly correlates with the change in film

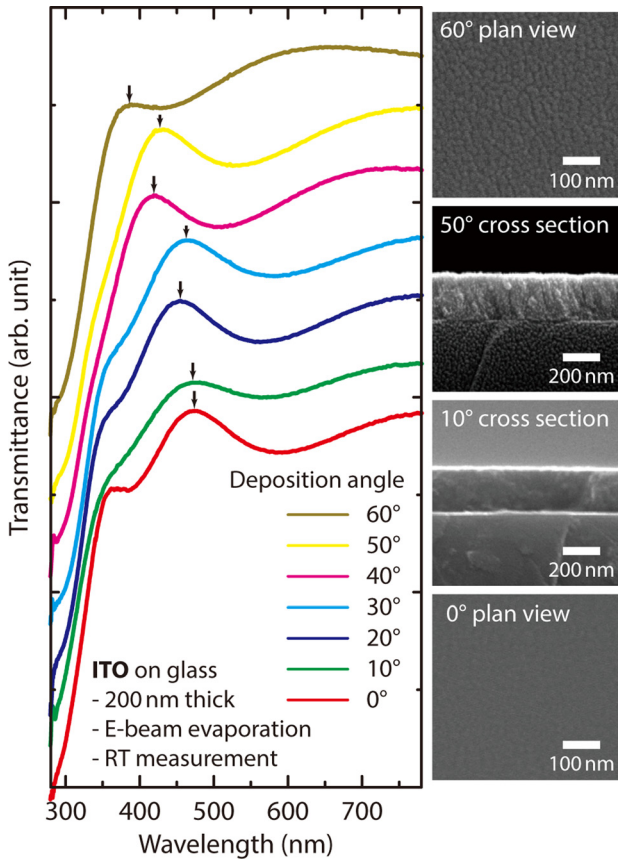


FIG. 2. Optical transmittance curves of the ITO thin films deposited at 0° to 60° tilt angles. Plan view and cross-sectional SEM images of the ITO films are shown on the right.

porosity, resulting in a change in the film's optical properties such as the refractive index.

Above all, the transmittance threshold, representing the optical bandgap of the ITO films, shifts toward longer wavelengths with the increasing tilt angle, indicating a decrease in the optical bandgap energy. There are several models and reports that correlate the optical absorption coefficient ($\alpha$) and optical bandgap energy ($E_g$) of a material.[14] In the present study, the Tauc method is utilized to estimate the optical bandgap values.[13] When a direct optical transition is assumed for the ITO samples, the optical bandgap energy can be quantitatively derived by[15]

$$\alpha h\upsilon \propto \beta(h\upsilon - E_g)^{1/2}, \tag{2}$$

where $\beta$ is a constant and $h\upsilon$ is the photon energy. Note that Eq. (2) can be applied to the spectral range where the change in absorption is strong. Figure 3 shows plots of $(\alpha h\upsilon)^2$ versus photon energy for all ITO films. The bandgap values of the films were deduced from the extrapolation of the linear range of the $(\alpha h\upsilon)^2$ versus $h\upsilon$ plots. It is notable that, as shown in the inset of Fig. 3, the optical bandgap *decreases* with the increasing tilt angle, which has not yet been reported for OAD films. The solid line in the inset of Fig. 3 is a linear fit to visually show the decrease in the bandgap energy. The ITO film deposited at a tilt angle of 10° has the maximum value of the optical bandgap, 4.02 eV, whereas the minimum value, 3.87 eV, belongs to the ITO film deposited at a 60° tilt angle. As shown in the literature,[16,17] the direct optical

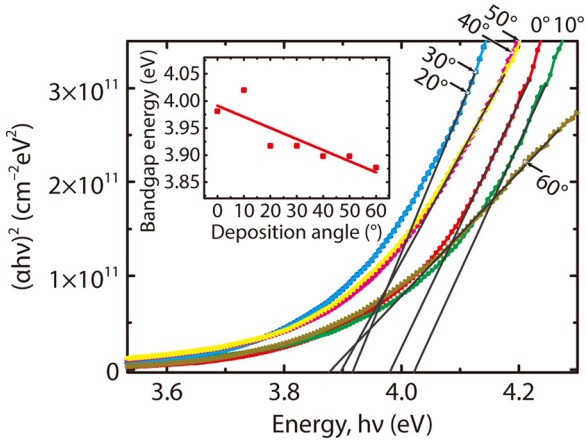


FIG. 3. $(\alpha h\upsilon)^2$ versus photon energy plots of the ITO thin films. (Inset) Bandgap energy of the films as a function of deposition angle, deduced from the extrapolation of the linear plots of $(\alpha h\upsilon)^2$ versus $h\upsilon$.

bandgap of the ITO thin films changes from 3.5 to 4.5 eV due to the degeneracy of semiconductor oxides, which has been explained by two competing mechanisms: (i) optical bandgap narrowing caused by electron–electron and electron–impurity effects in the valence and conduction bands, and (ii) optical bandgap widening due to blockage of the lowest states of the conduction band by excess electrons (Burstein–Moss effect). However, in our experiment, as the ITO fabrication procedure is identical for all ITO samples with the exception of the tilt angle, these hypotheses are insufficient in explaining the variation in optical bandgap shown in the inset of Fig. 3.

XRD technique can be used to determine the texture, grain size, interplanar spacing, and lattice constants of thin films. In order to investigate a potential microstructural change during the ITO deposition, the X-ray diffraction between 29° and 37° is measured for the ITO films grown on glass substrates, the results of which are shown in Fig. 4. The corresponding (hkl) Miller indices belonging to the $In_2O_3$ diffraction lines are also shown in the figure. Although the locations of the diffraction peaks (that include the compositional information of a material) for the (222) and (400) planes do not change considerably, the relative peak intensity between these planes significantly changes with the tilt angle used during ITO deposition.

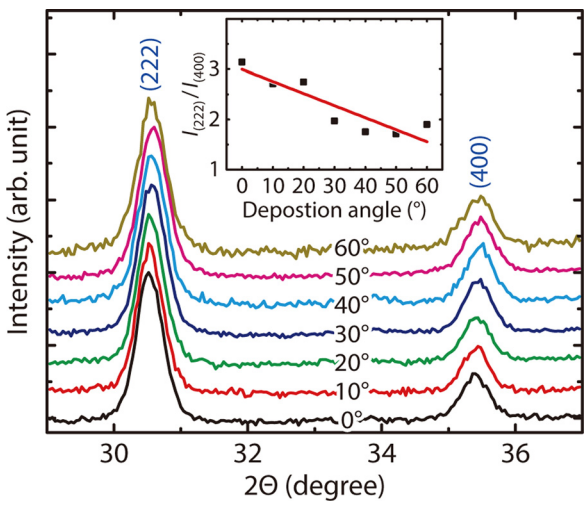


FIG. 4. X-ray diffraction patterns of the ITO films grown on glass substrates. (Inset) The $I_{(222)}/I_{(400)}$ values as a function of deposition angle.

The highest intensity (222) peak is obtained for the ITO sample deposited at 0°. The (400) peak becomes very strong with the increasing tilt angle as a result of the preferred orientation in the direction of ⟨100⟩. The ratio between the intensities of the (222) and (400) peaks is known as the crystal quality parameter.[18,19] The $I_{(222)}/I_{(400)}$ value is calculated for all ITO samples and plotted in the inset of Fig. 4. Note that the shape of the figure is very similar to that of the inset of Fig. 3. The ratio of the ITO sample deposited at 0° is approximately 3.14, which is near the standard value of 3.33 for ITO powder. Meanwhile, the ratio of the ITO sample at 60° is approximately 1.90 (the smallest value among the values determined), which is much less than the standard value of the ITO powder, indicating that most of the layer parallel to the film surface is textured in the ⟨100⟩ direction. The results of the XRD measurement indicate that the microstructure of the ITO film has a strong dependency on the tilt angle. Although the reason for this transition of the preferred growth direction is not obvious, it might be caused by the diffusion length variation of evaporated particles affected by a geometric surface structure.

Finally, the significant shift in the optical bandgap of ITO thin films shown in the inset of Fig. 3 is explained by the microstructural change made by the variation of the preferential growth direction of ITO particles. Generally, a microstructural modification can induce a change in the optical properties of a thin film. The change in preferred growth direction from ⟨111⟩ to ⟨100⟩ can lead to a stressed film due to a large mismatch in the film's lattice constant with the substrate's lattice constant.[18,20,21] The stress can stem from oxygen deficiency[22,23] and the mismatch in lattice constants or thermal expansion coefficients between the film and substrate.[24] In other words, the variation in optical bandgap energy observed in the present study might be caused by differences in growth-induced stress of ITO films.[25]

In conclusion, this study investigates the effect of tilt angle used during the OAD process on the microstructural and optical properties of ITO thin films deposited on silicon and glass substrates. With the variation in tilt angle, changes are found in the ITO's refractive index, porosity, and especially optical bandgap energy. With the increasing tilt angle, ITO films change to have a ⟨100⟩ preferential growth direction and are in the condition of increased strain at the interface between ITO and substrate, resulting in a decrease of optical bandgap energy. The ITO film optical bandgap varies from 3.98 eV (at normal deposition) to 3.87 eV (at a 60° tilt angle).

The authors gratefully acknowledge the support by the Basic Science Research Program through the National Research Foundation (NRF) of Korea funded by the Ministry of Education (2014R1A1A2054092 and 2015R1A6A1A04020421).

[1]A. Barranco, A. Borras, A. R. Gonzalez-Elipe, and A. Palmero, Prog. Mater. Sci. **76**, 59–153 (2016).
[2]K. D. Harris, A. C. van Popta, J. C. Sit, D. J. Broer, and M. J. Brett, Adv. Funct. Mater. **18**, 2147–2153 (2008).

[3]X. Yan, F. W. Mont, D. J. Poxson, J. Cho, E. F. Schubert, M. H. Kim, and C. Sone, J. Appl. Phys. **109**, 103113 (2011).
[4]P. Yu, C.-H. Chang, C.-H. Chiu, C.-S. Yang, J.-C. Yu, H.-C. Kuo, S.-H. Hsu, and Y.-C. Chang, Adv. Mater. **21**, 1618–1621 (2009).
[5]J.-Q. Xi, M. F. Schubert, J. K. Kim, E. F. Schubert, M. Chen, S.-Y. Lin, W. Liu, and J. A. Smart, Nat. Photonics **1**, 176–179 (2007).
[6]L. González-García, I. González-Valls, M. Lira-Cantu, A. Barrancoa, and A. R. González-Elipe, Energy Environ. Sci. **4**, 3426–3435 (2011).
[7]Y. Zhou, T. Taima, T. Miyadera, T. Yamanari, M. Kitamura, K. Nakatsu, and Y. Yoshida, Nano Lett. **12**, 4146–4152 (2012).
[8]R. Teki, M. K. Datta, R. Krishnan, T. C. Parker, T.-M. Lu, P. N. Kumta, and N. Koratkar, Small **5**, 2236–2242 (2009).
[9]R. Krishnan, T.-M. Lu, and N. Koratkar, Nano Lett. **11**, 377–384 (2011).
[10]N. A. Malvadkar, M. J. Hancock, K. Sekeroglu, W. J. Dressick, and M. C. Demirel, Nat. Mater. **9**, 1023–1028 (2010).
[11]D. J. Poxson, F. W. Mont, M. F. Schubert, J. K. Kim, and E. F. Schubert, Appl. Phys. Lett. **93**, 101914 (2008).
[12]J. K. Kim, S. Chhajed, M. F. Schubert, E. F. Schubert, A. J. Fischer, M. H. Crawford, J. Cho, H. Kim, and C. Sone, Adv. Mater. **20**, 801–804 (2008).
[13]J. Tauc, Mater. Res. Bull. **3**, 37–46 (1968).
[14]H. N. Cui, V. Teixeira, and A. Monteiro, Vacuum **67**, 589 (2002).
[15]J. I. Pankove, *Optical Processes in Semiconductors*, 2nd ed. (Dover Publications Inc., New York, 1970).
[16]J. F. Smith, A. J. Aronson, D. Chen, and W. H. Class, Thin Solid Films **72**, 469 (1980).
[17]M. J. Alam and D. C. Cameron, Thin Solid Films **377–378**, 455–459 (2000).
[18]E. Terzini, G. Nobile, S. Loreti, C. Minarini, T. Polichetti, and P. Thilakan, Jpn. J. Appl. Phys. **38**, 3448 (1999).
[19]C. V. R. Vasant Kumar and A. Mansingh, J. Appl. Phys. **65**, 1270 (1989).
[20]P. Thilakan, C. Minarini, S. Loreti, and E. Terzini, Thin Solid Films **388**, 34 (2001).
[21]A. Mohammadi Gheidari, F. Behafarid, G. Kavei, and M. Kazemzad, Mater. Sci. Eng. B **136**, 37 (2007).
[22]J. Ye and K. Nakamura, Phys. Rev. B **48**, 7554 (1993).
[23]S. Shin, Mater. Res. Bull. **16**, 299 (1981).
[24]W.-F. Wu and B.-S. Chiou, Thin Solid Films **293**, 244–250 (1997).
[25]L. Kerkache, A. Layadi, E. Dogheche, and D. Rémiens, J. Phys. D: Appl. Phys. **39**, 184 (2006).